Nucleic Acids Research, 1994, Vol. 22, No. 14 2845–2852

Site-specific targeting of psoralen photoadducts with a triple helix-forming oligonucleotide: characterization of psoralen monoadduct and crosslink formation

Francis P.Gasparro*, Pamela A.Havre[1], Gerard A.Olack, Edward J.Gunther[1] and Peter M.Glazer[1]

Departments of Dermatology and [1]Therapeutic Radiology, Photobiology Laboratory, Yale University, 15 York Street, New Haven, CT 06520-8059, USA

Received January 10, 1994; Revised and Accepted May 11, 1994

ABSTRACT

A polypurine tract in the *supF* gene of bacteriophage λ (base pairs 167 – 176) was selected as the target for triple helix formation and targeted mutagenesis by an oligopurine (5′-AGGAAGGGGG-3′) containing a chemically linked psoralen derivative (4′-hydroxymethyl-4,5′,8-trimethylpsoralen) at its 5′ terminus (psoAG10). The thymines at base pairs 166 and 167, a 5′ApT site, were targeted for photomodification. Exposure of the triple helical complex to long wavelength ultraviolet radiation led to the covalent binding of psoAG10 to the targeted region in the *supF* gene and to the induction of site-specific mutations. We report here experiments to characterize the photomodification of the targeted region of the *supF* gene in the context of triple helix formation. An electrophoretic mobility-shift assay showed that, at low radiation doses, monoadducts at base pair 166 were the major photoadducts. At higher doses the monoadducts were converted to crosslinks between base pairs 166 and 167. HPLC analysis of enzymatically hydrolyzed photoreaction mixtures was used to confirm the electrophoresis results. A strong strand preference for specific photoadduct formation was also detected.

INTRODUCTION

The facile synthesis of oligodeoxyribonucleotides (ODN) has led to an exponential growth of the antisense field in recent years. Antisense ODNs have been used to target RNA, single-stranded regions of DNA, or the single-stranded nucleic acids of some viruses via complementary base pair formation. ODNs can also be used to form triple helices with duplex DNA, since third strands, targeted to selected regions of double-stranded DNA, can bind with existing base pairs in the major groove by Hoogsteen and reverse Hoogsteen base pair interactions (1). In addition to physical chemical studies demonstrating the formation of triplex structures (2), studies in HeLa cells have shown that a triple helix-forming oligonucleotide targeted to the *c-myc* promoter reduced *c-myc* mRNA levels (3). In another study Roy (4) showed that a triple helix forming oligonucleotide (a 21 base oligopyrimidine) inhibited the transcription of an interferon responsive element in a plasmid that had been transfected into HeLa cells. A 38 base ODN with a high triplex binding affinity has been used to block the binding of the progesterone receptor to its target DNA sequence (5).

One important area of biological and structural chemistry has been the development of techniques to stabilize and prolong interactions between ODNs and the target nucleic acids (6,7). Thus, the linkage of DNA binding agents to ODNs has become a very popular strategy to enhance the efficacy of antisense and triplex inhibition of cellular processes. Helene *et al.* (8) first demonstrated that the thermodynamic interaction of ODNs and their nucleic acid targets was stabilized several fold by the covalent linkage of an intercalating agent (acridine orange) at the terminus of an ODN. Subsequently, several other agents have been employed with the most widely used compound being one of the furocoumarin family (psoralens) (9, 10). The tricyclic aromatic psoralens have two photoreactive carbon-carbon double bonds — the 4′,5′ bond in the furan ring and the 3,4 bond in the pyrone ring (11). These two heterocyclic rings are fused on either side of a benzene moiety resulting in a planar molecule with extended aromaticity possessing a strong tendency to intercalate with DNA base pairs. The photoactivation of psoralens with longwavelength ultraviolet radiation (320–400 nm, UVA) may lead to the 2+2 cycloaddition of either of its two photoreactive sites with 5,6-carbon bonds of pyrimidines. Depending on the extent of intercalation, other processes, including photodegradation of unbound psoralen and singlet oxygen formation may also occur. Several workers have demonstrated that furanside 4′,5′-monoadducts are competent precursors to crosslinks and pyroneside 3,4-monoadducts are not (12). In this report crosslink refers to the psoralen interstrand photoadduct bridging the target double-stranded region that results from the sequential absorption of two photons. In chemical terms monoadduct formation alone results in the crosslinking of the psoralen-linked ODN to one strand of the target. Although psoralens have been shown to react directly with all of the major DNA bases except G, the major focus of adduct characterization

*To whom correspondence should be addressed

has been on thymine photoadducts because they are the most abundant. Thus, in most studies, as in this report, thymine has been the target for photomodification.

Hearst and coworkers originally characterized the distribution of psoralen photoadducts (monoadducts and crosslinks) in synthetic polynucleotides and calf thymus DNA (13). Gasparro *et al.* (14) analyzed photoadduct formation in DNA isolated from cells (lymphocytes and keratinocytes) treated with 8-methoxypsoralen (8-MOP) and UVA. Sequence analysis has been used to demonstrate that the most reactive base sequence for psoralen photoaddition is the 5'TpA site (15). In cells, typical UVA irradiation conditions led to the formation of nearly equal amounts of monoadducts and crosslinks (16). More recently the selective photo-induction of 8-MOP monoadducts alone was achieved using visible light for photoactivation (17). Prior to the present study, psoralen photoadduct production as a result of third strand alignment had not been rigorously characterized.

Quantum efficiency studies for the photoreaction of the intercalated psoralen molecule indicated that the initial photoadduct quantum yield was 0.65% (18). The subsequent photo-conversion of these monoadducts to crosslinks was shown to be almost 5 times more efficient than the primary photoreaction (19). Although exact quantum yields for psoralens tethered to ODN have not been reported, recent experimental evidence indicates that the tethered compounds react efficiently (20). In addition, as a result of the specific targeting effect of the ODN, the stringent sequence dependence for photoreactivity (usually 5'TpA for free psoralen molecules) may be significantly reduced so that the usually less reactive 5'ApT site can be targeted (15).

Two different sites in psoralens have been employed for linkage to ODN. The commercial availability of psoralens containing primary amino groups (-NH2) or hydroxy groups (-OH) at the 4' carbon atom of the furan ring has led to the facile synthesis of psoralen tethered to ODN using commercially available bifunctional chemical crosslinking agents. Miller and coworkers (21) demonstrated that a 12 base ODN with a tethered psoralen (AMT) led to site-specific adduct formation in a single-stranded target DNA sequence. However, because the site of chemical addition to ODN involved the psoralen bond at which the most predominant photoadduct normally is formed (4',5'-MA), it was *assumed* that the reaction occurred at the usually less reactive 3,4 pyrone double bond. No chemical evidence was presented to support this interpretation. In more recent work, this group employed 3-carbethoxypsoralen (3-CPs) in which the carbethoxy group attached to the pyrone ring was linked to a tether, leaving the 4',5' furan bond available for efficient photoreaction with a target base (10). Three 21 base oligomers containing 3 variations in a crosslink site (AAT, ATA, TAA) were targeted with a 9 base oligomer with a CPs moiety at its 5' terminus.

Using another psoralen derivative, Helene and coworkers tethered 5-methoxypsoralen via a linker to the terminal 5' nucleotide in an 11 base ODN (9). It was anticipated that the primary photoreactions would occur at the unencumbered 4',5'-furan double bond. The dose-dependent formation of first a monoadduct linking the pso-ODN to one strand and then a second photoreaction that resulted in a crosslink was demonstrated by electrophoretic analysis. Although these results were consistent with the initial formation of 4',5'-monoadducts (and their subsequent conversion to crosslinks), no direct chemical evidence for the formation of 4',5'-monoadducts was presented. In subsequent *in vitro* studies with 5-MOP tethered to a 15mer, crosslinking to a triplex target site inhibited the expression of reporter plasmids transfected into a tumor T cell line (20).

We have used an ODN with a tethered psoralen (4'-hydroxymethyl-4,5',8-trimethylpsoralen, HMT) to site specifically induce DNA damage and thereby mutations in the *supF* gene contained within a λ phage vector grown in *E.coli* (22) and within a simian virus 40 vector in monkey cells (23). This is an approach designed to produce a permanent, heritable change in gene sequence and function as a possible form of genetic engineering or gene therapy. A homopurine-homopyrimidine sequence in the *supF* gene, adjacent to a 5'ApT site (see Figure 1), was selected as a site for triple helix formation by the purine motif (24). HMT was linked to the 5' end of the ODN (AGGAAGGGGG, hence psoAG10) via the 4'-hydroxymethyl group. Following triple helix formation, intercalation, and photoactivation of the psoralen, photoadduct formation was expected at base pairs 166–167. Analysis of the mutations induced in the λ vector by psoAG10 revealed greater than 500-fold specificity for the targeted *supF* gene in comparison with the non-targeted cI gene (λ repressor). Further, almost all of the mutations were found by DNA sequence analysis to be at or near the target site at bp 166–167, with 56% consisting of TA→AT transversions at bp 167. In contrast, a survey of mutations produced by free psoralen showed a scattered distribution of mutations, with none seen at bp 167 (22).

To account for the mutations induced by the psoralen-linked, triplex-forming ODN, we designed experiments to determine which photoadducts formed when psoAG10 was used to photomodify the *supF* gene target with UVA. We report here the distribution of photoadducts produced under the actual conditions of the targeted mutagenesis described previously. In contrast to previous studies, we did not rely on adduct distribution determined using free psoralen compounds. Rather we examined the formation of specific photoadducts formed when psoAG10 was used tophotomodify either the *supF* gene (246 base pairs (bp)) or a 24 bp fragment of the *supF* gene containing the psoAG10 target site. In the *supF* gene, the photoreaction products were analyzed by reversed phase HPLC after enzymatic digestion, and in the 24 bp duplex, by a mobility shift assay using gel electrophoresis. In a UVA dose study employing the 24 bp duplex we also show a shift in the distribution of adduct type as monoadducts formed at a low UVA dose at one site are converted to crosslinks at the neighboring site. A distinct strand preference for photoreaction with the purine-rich strand is also described. Although the distribution of psoralen photoadducts formed in the context of the triple helix environment varies to some degree from that formed in double stranded DNA, the adducts are chemically identical. However, the targeting by the triple helix forming psoAG10 appears to relax the preferential tendency for photoadduct formation to occur at 5'-TpA sites. In these studies we also describe the use of visible light (419 nm or 447 nm) to activate the psoralen moiety in psoAG10.

MATERIALS AND METHODS

Oligonucleotides/DNA substrates

Twenty-four base ODNs corresponding to the target region in the *supF* gene (see Figure 1, or to variations of it as shown in Figure 3) were prepared by solid phase synthesis. ODNs were end-labeled with T4 polynucleotide kinase (New England Biolabs, Beverly MA) and [γ-^{32}P]ATP (Amersham, Arlington Hts, IL). Labeled oligomers were separated from unincorporated

Figure 1. Strategy for triple helix formation with psoAG10. The sequence of the psoralen-linked oligopurine, psoAG10, is shown positioned opposite the target sequence binding site for triplex formation (bp 167–176) in the *supF* gene, an *E.coli* amber suppressor tRNA (29). The HMT moiety tethered at the 5' terminus was designed to react with thymidine at bp 167. Pu24: upper strand — purine-rich; Py24: lower strand — pyrimidine-rich. This 24 base pair duplex matches bp 160–183 of *supF* and represents ~10% of the entire *supF* gene.

[γ-^{32}P]ATP by passing the mixture through a G25 spin column (Boehringer-Mannheim, Indianapolis, IN). PsoAG10 (5'-AGG-AAGGGGG-3') was also prepared by solid phase synthesis with the psoralen (4'-hydroxymethyl-4,5',8-trimethylpsoralen, HMT) incorporated as a phosphoramidite (Oligos Etc, Wilsonville, OR and Glen Research, Sterling, VA).

PCR was used to prepare the [^{3}H-thymidine]*supF* 246 base pair double-stranded DNA fragment that was used to characterize photoadduct formation by HPLC analysis after phototreatment and enzymatic hydrolysis (see below).Asymmetric PCR was used to prepare individually labeled *supF* gene fragments (246 bases). In addition *supF* gene fragments with mutations near the targeted crosslink sites (e.g., such that the 5'ApT site was replaced with a p5'TpT site, not a crosslinking site) were used in additional experiments to assist in the characterization of the psoralen photochemistry.

Radiation sources

Fluorescent lamps emitting either UVA or visible light used in these studies were described previously (17). Briefly, UVA lamps emitting 320–400 nm radiation were used in conjunction with a window glass filter to eliminate UVB radiation (typical UVA irradiance 4 mW/cm^2). UVA doses were determined by radiometry (International Light, Newburyport, MA). Two types of fluorescent lamps emitting visible radiation at 419 nm and 447 nm were also used (Southern New England Ultraviolet Co, Branford, CT). The spectral distribution of these lamps was determined by focusing the light onto a Jarrell-Ash Monospec 27 (Allied Analytical, Waltham MA) equipped with an optical spectral multichannel analyzer and a diode array detector (Princeton Instruments, Princeton, NJ). An irradiance of 6.5 mW/cm^2 was determined using a calibrated silicon diode UV250BQ (EG&G, Montgomeryville, PA). A monochromator (PTI, Princeton NJ) equipped with a 75 W Xe arc lamp was used for 300 nm irradiations.

Electrophoretic analysis of phototreated 24 base pair *supF* target

24 bp duplex targets, either an exact subset of the *supF* gene (bp 160–183) or a set of target site mutations, were formed by annealing 150 ng of one unlabeled 24mer with a presumed equal amount of the labeled complementary 24mer (assuming 60% recovery after labelling and purification). Formation of the triplex was performed in a binding reaction for 2 hrs at 37°C using 0.35 picomoles (in 10 μL) of the double stranded target and 35 picomoles of psoAG10 in 10% sucrose, 20 mM $MgCl_2$, 10 mM Tris·Cl, pH 8.0, 1 mM spermidine.

Following triple helix formation, samples were exposed to visible light (447 nm) or UVA radiation for various times, and then denatured by adding 90 μL offormamide to each 10 mL reaction. Samples (30 μL) were analyzed on a 20% acrylamide, 7 M urea gel in 90 mM boric acid, 90 mM Tris, and 2 mM EDTA along with labeled markers (Pu24 and Py24, before and after annealing). The gels were run at 400 volts for 3 hrs, dried for 3 hrs and exposed to film (Kodak X-AR) for 1 hr. The gel in Figure 2 was also analyzed directly by phosphor-imaging (Molecular Dynamics, Sunnyvale, CA).

Photoadduct formation and analysis in *supF* gene fragment

To determine the extent and type of photoadduct formation by HPLC analysis, the 246 bp [^{3}H]*supF* duplex generated by PCR and psoAG10 were exposed to either visible light (419 nm or 447 nm) or UVA radiation. The initial photoreaction (monoadduct formation) of [^{3}H]thymidine-*supF* with psoAG10 was performed on 10 μL aliquots using the conditions described above at 419 nm for 30 min. Water droplets (10 μL) were added to the sealed petri dish to minimize evaporation from the reaction solution. Unreacted psoAG10 was removed using a Centricon-100 filter (sample diluted to 2 ml with H_2O, centrifuged, diluted to 2 ml and centrifuged again). Buffer was added to the sample, and 10 μL aliquots were irradiated with UVA for 5 min to convert psoralen monoadducts to crosslinks. After the UVA treatment, an aliquot was diluted 10 fold with H_2O. To photoreverse the crosslinks, the solution was irradiated at 300 nm for 5 min (20 nm bandpass) using a single grating monochromator. Aliquots were removed after each irradiation step for enzymatic hydrolysis and HPLC analysis (see below).

Photoadduct quantitation and distribution

To quantify the conversion of the thymines to psoralen–thymine photoadducts, the [^{3}H]thymidine-labeled DNA was hydrolyzed using nucleolytic enzymes (nuclease P1, DNase I) and then analyzed by reversed phase HPLC as described in a previous report (16). A Microsorb-MV 4.6×250 mm C-18 reversed phase HPLC column (Rainin, Woburn, MA) was used in conjunction with an SP8800 ternary HPLC pump (Spectra Physics, San Jose, CA) equipped with a forward optical scanning detector (200–360 nm) and a software package for data analysis. A mobile phase consisting of methanol (A) and 0.1 Mtriethylammonium acetate, pH 6.8 (B) at a flow rate of 1 ml/min with a linear gradient (time 0, 5.5% A; time 0.1, 9.0% A; time 3.5, 15.7% A; and time 40, 60% A) was used to elute the photomodified *supF* components. To each 0.5 ml fraction 4 ml scintillation fluid (Ecoscint, National Diagnostics, Manville, NJ) was added prior to scintillation analysis (LKB Rack Beta). As with other psoralen photoadducts we have characterized, HPLC analysis showed new species eluting later than thymidine (due to the hydrophobicity of the psoralen moiety). Aliquots were removed after each photochemical step. The late-eluting species (fractions 30–80) were characterized by analyzing the pattern of these photoadduct species after either monoadduct conversion to crosslinks (with UVA) or crosslink photoreversal (with 300 nm radiation). Individually labeled 246 base *supF* strands were used in another

series of experiments to characterize the nature of photoadducts formed on *each* strand.

Quantitative preparation of photoadducts

The [^{3}H]*supF* was reacted with psoAG10 in quantity (fourteen 10 μL aliquots) under standard conditions with 5 min of UVA. The aliquots were combined, hydrolyzed, and analyzed by HPLC (gradient to 50% A). Fractions corresponding to new species (as detected by late-eluting ^{3}H counts) were collected and reanalyzed by HPLC. None of these fractions contained unmodified thymidine. After lyophilization and resuspension, the purified psoralen photoadducts were also characterized on the basis of their sensitivity to 300 nm irradiation (5 min).

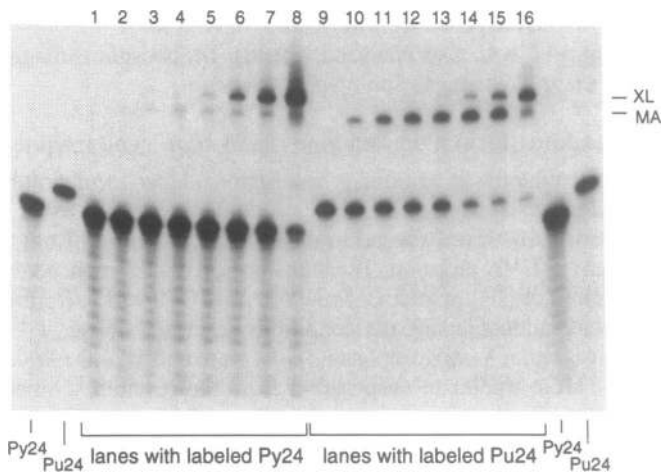

Figure 2. Denaturing mobility-shift assay: Photobinding of psoAG10 to 24 bp *supF* target sequence. Polyacrylamide gel electrophoresis was performed under denaturing conditions to analyze the photobinding of psoAG10 to the 24 bp duplex target. Lanes labeled Pu24 and Py24 represent untreated 24mer duplex in which one complementary strand was end labeled with ^{32}P. Lanes 1–8 contained labeled Py24 incubated in the presence of unlabelled Pu24 plus psoAG10. Lane 1, dark control; lanes 2–4 were exposed to 3.9, 7.8 and 11.7 J/cm^2 447 nm light; lanes 5–8 were exposed to 0.029, 0.086, 0.171 and 1.71 J/cm^2 UVA radiation. Lanes 9–16 contained labelled Pu24 plus unlabelled complementary Py24 and psoAG10. Lane 9, dark control; lanes 10–12 were exposed to 447 nm light and lanes 13–16 to UVA (as described for Py24). The photobinding of psoAG10 as a result of the photoactivation of the psoralen moiety retarded the migration of the 24 base pair oligomers. The position of the monoadducted oligomers (psoAG10 plus one of the 24mer oligonucleotides) is labeled MA; that for crosslinked strand (psoAG10 plus 24mer duplex)is labeled XL. At the highest UVA dose (1.71 J/cm^2) 67% of the adducts were crosslinks, while at the highest 447 nm dose only 3.3% of the adducts were crosslinks. Note: XL=crosslink, MA=monoadduct.

RESULTS AND DISCUSSION

The strategy we employed for triple helix formation using psoAG10 is depicted in Figure 1 in which the 10 base sequence of a psoralen-linked oligopurine is positioned opposite the target sequence binding site for triplex formation (bp 167–176) in the *supF* gene. In this motif, the homopurine strand binds antiparallel to the purine-rich strand (24).The HMT moiety was tethered with a two carbon linker to the 5′ terminus of the oligopurine so that the psoralen moiety could react with thymidines at bp 166–167.

Figure 2 shows the autoradiogram obtained from the denaturing PAGE analysis of the photoreaction of psoAG10 with the 24 bp target region of the *supF* gene (see Figure 1). In one set of experiments, the pyrimidine-rich strand (Py24) was end-labeled with [γ-^{32}P]ATP (left panel) and in another, the purine-rich strand (Pu24) was labeled (right panel). PsoAG10 was photoactivated with either 447 nm light (lanes 2–4 and 10–12 in the left and right panels, respectively) to determine whether strand-specific monoadduct formation could be induced or with UVA radiation (lanes 5–8 and 13–16, in the left and right panels, respectively) to induce crosslink formation (predominantly).

Considering the results of the 447 nm activation of psoAG10 first, a new autoradiographic band (MA) can be seen in lanes 2–4 and 10–12 corresponding to 10, 20 and 30 min doses of 447 nm light (3.9, 7.8 and 11.7 J/cm^2, respectively). The samples in lanes 1 and 9 were not irradiated. The yields of monoadducts and crosslinks, determined by direct phosphorimaging, are summarized in Table 1. The strand modification resulting from exposure to 447 nm light is shown. These data illustrate the strong preference of psoralen to react with the purine-rich strand which suggests that in the *supF* gene monoadduct formation occurs primarily at the thymidine at bp 166. In addition, a low level of crosslinking (in the range of 2–4%) was detected .

When UVA was used to photoactivate psoAG10, the reaction still favored the purine-rich strand (11:1 over the pyrimidine-rich strand). A dose-dependent increase in the extent of crosslink formation (presumably between T-166 and T-167) was observed

Table 1. Phosphorimaging analysis of psoAG10:24 bp duplex photoreaction

Radiation	Dose J/cm^2	Monoadducts* Pyr	Pur	Crosslinks Pyr	Pur
	0	0.609	0.334	0.869	1.62
447 nm	3.9	0.771	16.5	0.999	0.903
	7.8	1.03	29.8	1.11	1.03
	11.7	1.05	40.5	1.21	1.43
UVA	0.029	1.75	40.9	2.80	3.29
	0.066	–	57.0	–	12.0
	0.086	2.99	56.9	11.71	12.40
	0.17	3.66	51.9	22.8	25.1
	0.20	–	50.0	–	31.1
	0.90	–	23.2	–	54.0
	1.7	8.72	22.4	62.4	64.1

*Note: adduct yields are expressed an a percentage of the total signal. The sum of MA-Pyr, MA-Pu, either XL band and unreacted species(not listed) is ~100%.

regardless of which strand was labeled (Figure 3). As the band representing the crosslinked species increased (■— Pu24-XL; note that the band for Py24-XL (not shown) would parallel the band for Pu24-XL), the accompanying Pu24-MA band increased initially and then decreased (●) which is consistent with the Pu24-MA being converted to XL. The Py24-MA band reached a low level plateau value and did not change (▲). The conversion of MA to XL is consistent with experiments in which free psoralen compounds were used to photomodify DNA (16,18). These data also show that monoadducts formed on the pyrimidine-rich strand (presumably at bp 167) do not appear to be converted to crosslinks.

In order to support our interpretations of the gel mobility-shift data, we investigated triple-helix-directed photoadduct formation in 24 bp duplexes containing mutations at base pairs 165, 166, and 167 (Figure 3). These mutations eliminate the crosslinkable 5'ApT site at bp 166 and 167 by creating either a 5'TpTpT site at bp 165−167 (ODN 3 and 4) or a 5'ApApA site at bp 165−167 (ODN 5 and 6). In Figure 3, lanes 1−6 illustrate the mobility of the 5'-end labelled ODN. Lanes 7 and 8 show the products psoAG10 incubated with ODN 1 and 2 (the original Py24 and Pu24 shown in Figures 1 and 2) and activated with 0.2 J/cm^2 UVA. When ODN 1 (Py24) is labelled (lane 7) mostly crosslinks and not monoadducts are seen. This result duplicates the data presented in Figure 2 in which monoadducts are preferentially formed on the thymidine in bp 166 present in ODN 2 (unlabelled). When ODN 2 (Pu24) is labelled, both monoadducts and crosslinks are seen after a UVA dose of 0.2 J/cm^2. This, again, is consistent with the data presented in Figure 2. However, when ODN 3 and 4 are used to form a target duplex (lanes 9 and 10), no band corresponding to the presumed crosslink species is seen, consistent with the predicted absence of a crosslinkable site. Monoadducts are seen when ODN 3 is labelled (lane 9) but not when ODN 4 is labelled (lane 10). This suggests monoadducts are forming on the thymidine(s) in ODN 3 (at bp 165−167) but not on the adenine(s) in ODN 4. Similarly, no crosslinks are visualized when ODN 5 and 6 are used to form the duplex target (lane 11 and 12). Monoadducts are seen only when ODN 6 is labelled (lane 12) since this strand has thymidines at bp 165, 166, and 167. When ODN 5 containing adenines at bp 165−167 is labelled, MA are not identified. The slightly increased mobility of MA in lane 9 (psoAG10 linked to ODN 3) reflects the lesser molecular weight of ODN 3 (pyrimidine-rich) versus either ODN 2 or ODN 6 (both purine-rich).

To support and further elaborate the band assignments in the gel we used HPLC to analyze the types of photoadducts formed when the [^{3}H]*supF* gene (246 bpduplex) and psoAG10 were exposed to 30 min of 419 nm light. Overall adduct formation was 0.52% which is 59% of the expected level of modification if all of the targeted Ts at 166 and 167 were modified. In Figure 4 panel A shows the HPLC elution profile of the enzymatic hydrolysis mixture. The deoxyribonucleosides eluted in the following sequence dG, dC, dT, and dA from 9 to 12 min. New peaks due to the photoaddition of psoAG10 are not evident because the extent of photomodification of all the thymines (114) in the total DNA sample is very low (the maximum, if every targeted T were photomodified, would be 0.88%). To detect these species, 0.5 ml fractions were collected and analyzed by scintillation analysis. In all of the following panels in this figure, CPM (as a percentage of the total ^{3}H-thymidine, hence %CPM) is plotted versus fraction number. The profile shown in panel B was obtained from the 419 nm-irradiation reaction mixture. The large peak near fraction 20 corresponds to unmodified T (note the different scales: left for T; right for photoadducts). The predominant peak at fraction 72 corresponds to 4',5'-MA,

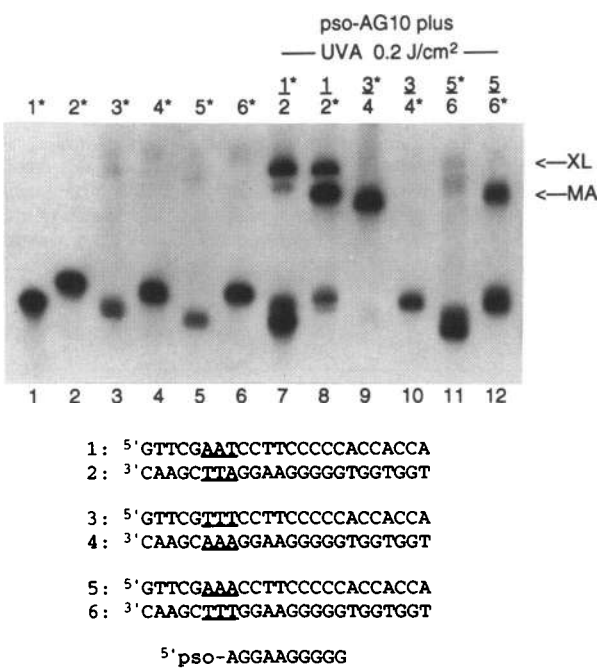

Figure 3. Denaturing gel mobility-shift assay: Photobinding of psoAG10 to mutant target sites. A series of 24 bp target duplexes were constructed by annealing synthetic ODN 1 and 2, 3 and 4, and 5 and 6. ODN 1 and 2 correspond to Py24 and Pu24, exactly matching the sequence of the *supF* gene. ODN 1 and 2 contain the crosslinkable 5'ApT site at bp 166−167. ODN 3 and 4 and ODN 5 and 6 are mutated at position 165−167 as indicated by the underlining. Lanes 1−6: labelled ODN 1*−6*, respectively. In lanes 7−12, the labelled ODN (*) was annealed to the complementary unlabelled ODN, incubated with psoAG10, and irradiated with 0.2 J/cm^2 UVA. The samples were analyzed by denaturing gel electrophoresis and autoradiography. The XL (both strands of the duplex covalently linked to psoAG10) and MA (one strand of the target duplex covalently linked to psoAG10) are indicated.

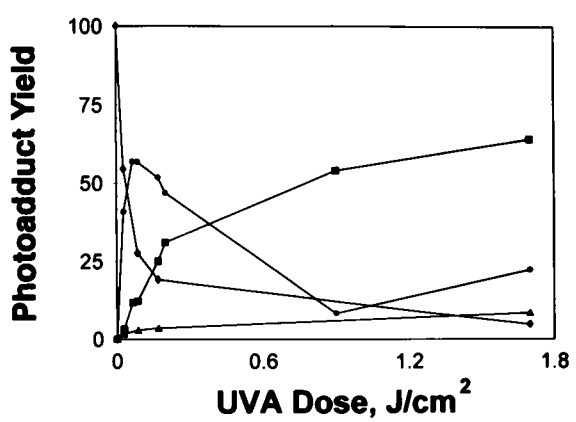

Figure 4. Yield of psoAG10-24mer species after exposure to UVA radiation (data corresponds to gel shown in Figure 2). Phosphor imaging intensity (%) for each photomodified band is plotted versus the UVA dose. (■ − Pu24-XL, ● − Pu24-MA. ▲ − Py24-MA, ◆ − unmodified Pu24).

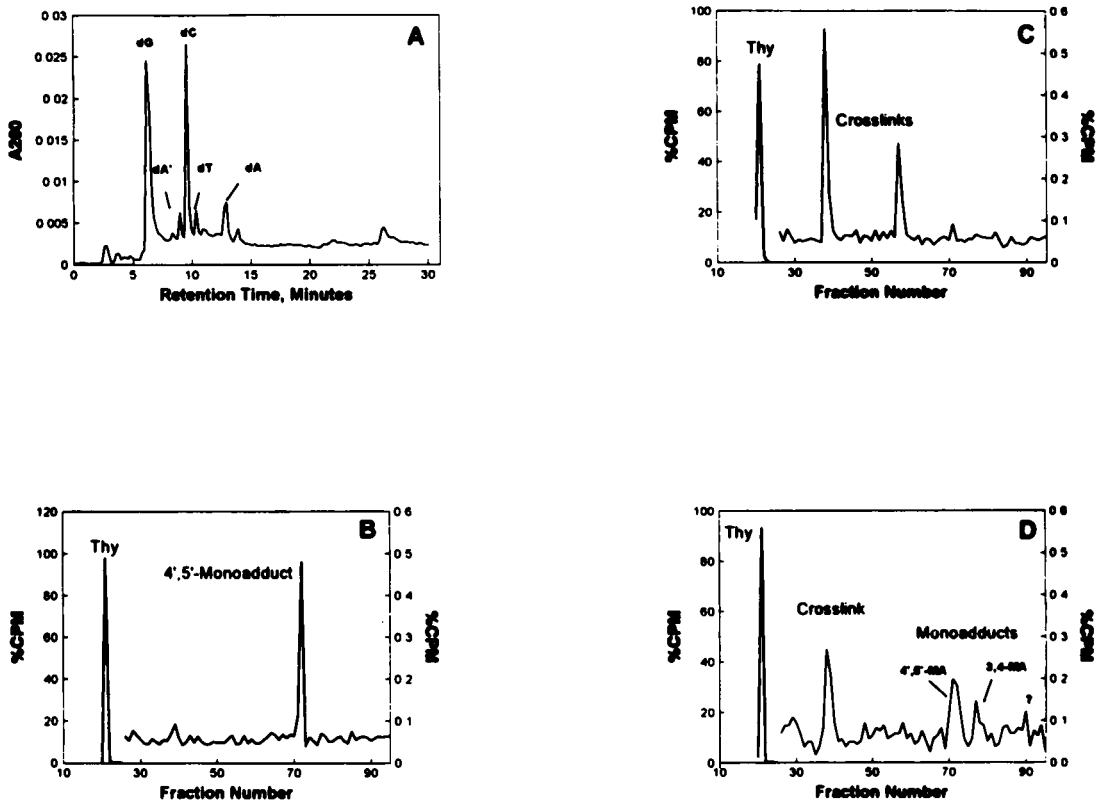

Figure 5. HPLC analysis of [^{3}H]*supF* DNA after photoreaction with psoAG10. (**A**) Elution profile of hydrolyzed DNA mixture monitored at 260 nm (only unmodified DNA components are evident by optical detection). Peaks corresponding to dG, dC, dA and dT are shown (dA', deaminated dA). Note that in the following CPM plots, different axes are used for thymidine (left 0–100%) and for the photoadducts (right 0–0.6%). %CPM refers to the percentage of the total ^{3}H-thymidine counts and corresponds to amount of a specific photoadduct species. (**B**) %CPM vs. fraction number for 0.5 ml fractions collected during HPLC analysis shown in (A). The primary photoadduct (4',5'-monoadduct) eluted in fraction 72; 0.52% of all thymines in the *supF* gene were modified: 87% monoadducts, 13% crosslinks. (**C**) %CPM vs. fraction number – photoconversion of 4',5'-monoadducts in the original 419 nm irradiated solution by a secondary exposure to UVA radiation (5 min); new adduct distribution: 8% monoadducts, 92% crosslinks. Notice reduced signal in fraction 71 (4',5'-MA) and the appearance of new species in fractions 38 and 57. (**D**) %CPM vs. fraction number – photoreversal of crosslinks; new adduct distribution: 52% 4',5'-monoadducts, 30% crosslinks and 19% 3,4-monoadduct. See text for complete discussion of peak assignments. The peak marked with '?' represents ~1% of the reaction mixture.

typically the primary psoralen photoadduct (11,13,16). In a second irradiation step after unreacted psoAG10 was removed by centrifugation through a Centricon-100 spin column, an aliquot of the original reaction mixture was exposed to UVA in order to convert 4',5'-MA to crosslinks. In Panel C it is seen that the species in fraction 72 was diminished and new species appeared in fractions 38 and 57. This sequence of photochemical events is consistent with the species in fraction 72 being identified as a 4',5'-MA and hence those in 38 and 57 as crosslinks (Note: in studies with 8-MOP and AMT we have shown that multiple peaks corresponding to the same type of photoadduct can arise due to pyrone ring opening). Another aliquot of the solution which had been initially exposed to 419 nm light and then UVA was diluted 10 fold and then exposed to 300 nm radiation to photoreverse the putative crosslinks to monoadducts and free thymidine (Panel D). The species in fractions 38 and 57 decreased, which is consistent with their assignment as crosslinks (25) while new species appeared in fractions 71 and 77 (4',5'-MA and 3,4-MA respectively). The elution order of these adducts (XL, 4',5'-MA, 3,4-MA) is consistent with results obtained for free psoralen crosslinks and monoadducts (16, 26). Thus, the direct analysis of the photoadducts and the results of the

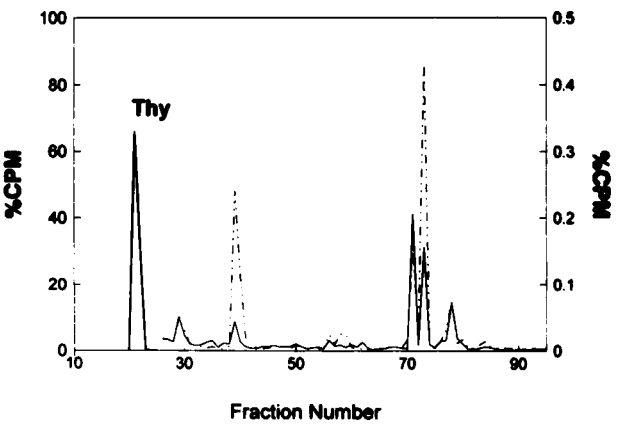

Figure 6. Comparison of HPLC analyses for wild type and mutant *supF* DNA. CPM vs. fraction number – adduct formation in mutant *supF* (solid line) exposed to UVA compared to that for wild type *supF* (broken line). In the wild type *supF* 65% of the adducts were crosslinks while in the mutated *supF*, (with a crosslinking site 1 bp away from the optimal site) the crosslink yield was only 14%. Note: as in Figure 6 there are different scales for T and photoadducts.

monoadduct induction–crosslink conversion and reversal experiments support the interpretation of the gel electrophoresis results described above. These experiments clearly show that the 4',5'-monoadduct was the major photoadduct (at lower doses) in spite of the attachment to the oligonucleotide *via* the 4'-carbon atom in the furan ring. It is important to note that we do not know if the photoadducts detected by HPLC analysis contain a portion of the linker arm. However, the data and adduct assignments presented above are consistent with the results we have obtained for 8-MOP (16) and AMT (26) photoadducts. In the latter case, we purified sufficient amounts of each major photoadduct to permit mass spectral analysis.

In an additional experiment we examined the strand dependence for the psoralen photoreaction. Photoreactions were performed in which only one strand (either purine-rich or pyrimidine-rich) was labeled with [^{3}H]thymidine. The strand-specifically labelled *supF* substrates were produced by annealing the reaction products from asymmetric PCR reactions. In these reactions, a 100-fold excess of one PCR primer was used to predominantly generate just one of the two strands (either ^{3}H-labelled or unlabelled). In this way, specific photomodifications of one strand or the other could be separately detected. Solutions of [^{3}H]*supF*(pur):*supF*(pyr) with psoAG10 and *supF*(pur):[^{3}H]*supF*(pyr) with psoAG10 were exposed to 419 nm, hydrolyzed and analyzed by HPLC. The photoreaction favored the purine strand by a factor of 9.3 which is in close agreement with the factor of 11 determined by the mobility shift assay using the 24 bp target sequence (see above). In the [^{3}H]*supF*(pur):*supF*(pyr) reaction 83.6% of the adducts were 4',5'-monoadducts while in the *supF*(pur):[^{3}H]*supF*(pyr) reaction 100% of the adducts were 3,4-monoadducts. This difference in the type of monoadduct generated on the pyrimidine-rich versus the purine-rich strand may explain our observation in the gel mobility-shift experiments (Figure 2 and Table 1) that the monoadducts on Pu24 were converted to crosslink but those on Py24 were not. The combined data suggest that primarily 4',5'-furanside monoadducts are produced on the thymidine at bp 166 in Pu24 and that these are readily converted to crosslinks with the thymidine at bp 167. In contrast, the monoadducts generated on the thymidine in bp 167 in Py24 aremainly 3,4-pyroneside monoadducts which undergo minimal, if any, conversion to crosslinks (13,16,26).

PsoAG10 and mutant *supF* DNA, in which the 5'ApT site was replaced with a 5'TpT site, were also exposed to UVA (Figure 6). In the mutant *supF* DNA 0.63% of the thymidines were modified as opposed to 0.72% in the wild type *supF* DNA. Since a TpT sequence is not usually considered a very reactive site (15), this result is indicative of the strong site-directing effects of the ODN. HPLC analysis showed that the vast majority of photoadducts were monoadducts (86% for the mutant *supF* vs. 35% for the wild type). The crosslink formation detected in the mutant *supF* (14%) may have arisen from a somewhat less favorable interaction of psoAG10 in which the psoralen moiety was able to intercalate between bp 165 and 166 to produce a crosslink between the thymidines at the 5'ApT site in this mutant *supF* gene.

Because psoAG10 was designed to target the thymidine in a 5'ApT site (on the Py24 strand at bp 167), the high efficiency for crosslink formation was also somewhat surprising since crosslinks normally form more efficiently at 5'TpA sites (15). Also it was expected that the chemical link at the 4'-hydroxymethyl position might interfere with efficient photoreaction at the 4',5' bond. These results showing that the photoreaction at the 4',5' bond in the furan ring is virtually unaffected by the linkage to the oligonucleotide indicate that previously published assumptions about psoralen photoreactivity in a similar environment may need re-evaluation (21). The tendency for psoralen photoreactions to occur preferentially at 5'TpA sites is based on studies of free psoralens with synthetic polynucleotides and calf thymus DNA. Much more powerful analyses of the photoreactivity of psoralens has now become possible by using synthetic ODN of defined sequences. Reactivity in terms of adduct formation, as well as the identity of adducts, can be determined by HPLC analysis (27).

The studies reported here have been performed using *in vitro* conditions under which triplex formation is highly favored due to the small size of the DNA containing the target duplex (either 24 bp in the *supF* fragment or 246 bp in the entire *supF* gene). However, in preliminary studies we have shown that psoAG10 is capable of binding to its target sequence in the genomic DNA of mouse cells containing integrated λ vector DNA (28 and Gunther *et al.*, in preparation). Similarly, Strobel *et al.* (29) showed that a 16 base oligopyrimidine (mCmCTTT(mCT)5C) was able to locate the 16 bp target site contained within the 3 Gbp of genomic DNA.

These studies have shown that the sequence specificity of triplex formation can be imparted to tethered chemical reagents in order to produce targeted DNA adducts and mutations. Photoactivatable reagents are highly desirable due to the controlling effects of light exposure. The further development of this field will hinge in part on the ability to extend the range of sequences available for third strand formation. The development of 'neutral' bases like 7,8-dihydro-8-oxoadenine (30) and 2'-deoxynebularine (31) offer the potential of tolerating interruptions in the homopurine or homopyrimidine runs at target sites. Since oligonucleotides are generally viewed as pharmacologic agents of the future, techniques such as those described in this report designed either to stabilize interactions between ODNs and their target nucleic acids or to produce permanent, heritable changes in the target DNA via induced mutations may hasten further developments in this field.

ACKNOWLEDGEMENTS

The authors thank Dr. Shawn O'Malley for his assistance in the spectrofluorometry experiments and John Scott who measured the output of the 447 nm lamps. This study was supported in part by an NIH Skin Disease Research Center Award (P01-AR41992-FPG and PMG) as well as grants to PMG from the NIH (ES05775), the Charles E. Culpeper Foundation and the Leukemia Society of America.

REFERENCES

1. Sun J-S. & Helene, C. (1993) *Curr. Opinion Struct. Biol. 3*, 345–356.
2. Maher, L.J., Dervan, P.B. & Wold, B. (1990) *Biochem. 29, 8820–8826.*
3. Postel, E.H., Flint, S.J., Kessler, D.J., & Hogan, M.E. (1991) *Proc. Natl. Acad. Sci., U.S.A. 88*, 8227–8231.
4. Roy, C. (1993) *Nucl. Acids Res. 21*, 2845–2852.
5. Ing, N.H., Beekman, J.M., Kessler, D.J., Murphy, M., Jayaraman, K., Zendegui, J.G., Hogan, M.E., O'Malley, B.W. & Tsai M-T. (1993) *Nucl. Acids Res. 21*, 2789–2796.
6. Helene, C. (1993) *Curr. Opinion Biotech. 4*, 29–36

7. Asseline U., Thuong, N.T., & Helene, C. (1983) *C. R. Acad. Sc. Paris 297*, 369–372.
8. Helene, C., Montenay-Garestier, T., Saison, T., Takasugi, M., Toulme, J.J., Asseline, U., Lancelot, G., Maurizot., J.C., Toulme, F., & Thuong, N.T.(1985) *Biochimie 67*, 777–783
9. Takasugi, M., Guendouz, A., Chassignol, M., Decout, J.L., Lhomme, J., Thuong, N.T., & Helene, C. (1993) *Proc. Natl. Acad, Sci., U.S.A. 88*, 5602–5606.
10. Bhan, P. & Miller, P.S. (1990) *Bioconj. Chem. 1*, 82–88.
11. Cimino, G.D., Gamper, H.B., Isaacs, S.T., & Hearst, J.E. (1985) *Ann. Rev. Biochem. 54*, 1151–1193.
12. Gasparro, F.P., Saffran, W.A., Cantor, C. R. & Edelson, R.L. (1984) *Photochem. Photobiol. 40*, 215–219.
13. Kanne, D., Straub, K., Hearst, J.E., & Rapopott, H. (1982) *J. Am. Chem. Soc. 104*, 6754–6764.
14. Gasparro, F.P., Bevilacqua, P.M., Goldminz, D., & Edelson, R.L. (1990) in *DNA Damage and Repair in Human Tissues* (Sutherland, B. & Woodhead, A. Eds.) pp 137–148, Plenum Press, NY.
15. Sage, E. & Moustacchi, E. (1987) *Biochem. 26*, 3307–3314.
16. Olack, G.A., Gattolin, P., & Gasparro, F.P. (1993) *Photochem. Photobiol. 57*, 941–949.
17. Gasparro, F.P., Gattolin, P., Olack, G.A., Deckelbaum, L.I., & Sumpio, B.E. (1993) *Photochem. Photobiol. 57*, 1007–1010.
18. Tessman, J.W., Isaacs, S.T., & Hearst, J.E. (1985) *Biochem. 24*, 1669–1676.
19. Shi, Y. & Hearst, J.E. (1987) *Biochem. 26*, 3792–3798.
20. Grigoriev, M., Praseuth, D., Guieyesse, A.L. , Robin, P., Thuong, N.T., Helene, C., & Harel-Bellan, A. (1993) *Proc. Natl. Acad. Sci., U.S.A. 90*, 3501–3505.
21. Lee, B.L., Murakami, A., Blake, K.R., Lin, S., & Miller, P.S. (1988a) *Biochem. 27*, 3197–3203.
22. Havre, P.A., Gunther, E.J., Gasparro, F.P., & Glazer, P.M. (1993) *Proc. Natl. Acad. Sci., U.S.A. 90*, 7879–7883.
23. Havre, P. A. and Glazer, P. M. (1993) *J Virology 67*, 7324–7331.
24. Beal, P.A. & Dervan, P.B. (1991) *Science 251*, 1360–1363.
25. Cimino, G.D., Shi, Y., & Hearst, J.E. (1986) *Biochem. 25*, 3013–3020.
26. Oroskar, A., Olack, G., Peak, M.J. & Gasparro, F.P. (manuscript submitted).
27. Gasparro, F. P., Edelson, R. L., O'Malley, M. E., Wong, H.H., & Ugent, S. J. (1991) *Antisense Res & Dev 1*, 117–140.
28. Glazer, P.M., Sarkar, S.N., & Summers, W.C. (1986) *Proc. Natl. Acad. Sci., USA 83*, 1041–1044.
29. Strobel, S.A., Doucette-Stamm, L.A., Riba, L., Housman, D.E. & Dervan, P.B. (1991) *Science 254*, 1639–1642.
30. Jetter, M.C. & Hobbs, F.W. (1993) *Biochem. 32*, 3249–3254.
31. Stilz, H.U. & Dervan, P.B. (1993) *Biochem. 32*, 2177–2185.